



# CO hydrogenation over a hydrogen-induced amorphization of intermetallic compound CeNi<sub>2</sub>

Naruki Endo<sup>a,\*</sup>, Shin-ichi Ito<sup>b</sup>, Keiichi Tomishige<sup>a</sup>, Satoshi Kameoka<sup>c</sup>, An Pang Tsai<sup>c,d</sup>, Toshiya Hirata<sup>d</sup>, Chikashi Nishimura<sup>d</sup>

<sup>a</sup> Graduate School of Engineering, Tohoku University, Aoba-yama 6-6-02, Sendai 980-8579, Japan

<sup>b</sup> Graduate School of Pure and Applied Sciences, University of Tsukuba, Tennodai 1-1-1, Tsukuba 305-8573, Japan

<sup>c</sup> Institute of Multidisciplinary Research for Advanced Materials (IMRAM), Tohoku University, 2-1-1 Katahira, Aoba-ku, Sendai 980-8577, Japan

<sup>d</sup> National Institute for Materials Science (NIMS), Sengen 1-2-1, Tsukuba 305-0003, Japan

## ARTICLE INFO

### Article history:

Received 1 July 2010

Received in revised form

14 November 2010

Accepted 17 November 2010

Available online 14 December 2010

### Keywords:

Hydrogen-induced amorphization (HIA)

Intermetallic compound CeNi<sub>2</sub>

Amorphous

CO hydrogenation

## ABSTRACT

CO hydrogenation over a CeNi<sub>2</sub>, an amorphous CeNi<sub>2</sub>H<sub>x</sub> and a disproportionate mixture containing Ce hydride and CeNi<sub>5</sub> which were prepared by hydrogen absorption, has been investigated. Catalytic properties are different among the three samples since the bulk structure of the samples changes during the reaction. Nevertheless, the amorphous CeNi<sub>2</sub>H<sub>x</sub> exhibits high activity as well as unique selectivity of hydrocarbons. This study shows that hydrogen-induced amorphization (HIA) is a potential activation treatment for intermetallic compounds for catalysts.

© 2010 Elsevier B.V. All rights reserved.

## 1. Introduction

Some intermetallic compounds (IMCs) have attracted much interest/attention in the field of catalysis [1,2]. This is due to the fact that atoms in an IMC orderly occupy definite positions with a strict stoichiometric composition, performing their new catalytic function in comparison with metallic elements as new potential for catalysis [3,4] or precursors of catalysts [5,6]. There are many unique IMCs with different structures (L1<sub>2</sub>, D0<sub>19</sub>, C23, B8<sub>2</sub>, C15), which can transform into the amorphous state by hydrogen absorption [7] i.e., hydrogen-induced amorphization (HIA). HIA has high potential to prepare catalysts with full or partial amorphous structure by controlling volume fraction of the amorphous structure arbitrarily. Thus, HIA for IMCs could provide a new path for synthesizing catalysts since many IMCs contain catalytically active elements such as Fe, Co, Ni and Rh etc. Additionally, the conditions of HIA are varied according to the alloy systems from low hydrogen pressure at room temperature for several hours to high pressure (>5 MPa H<sub>2</sub>) at ~450 °C for several days [8], allowing to choose any IMC suitable for a specific catalytic reaction. On the other hand, the IMCs after hydrogen absorption show several different struc-

tures; crystalline state, amorphous state and disproportionation, i.e. decomposition into a metal hydride and a pure metal (or an IMC) [7,8]. Thus, it is of particular interest to compare the catalytic properties of each structure.

On the other hand, amorphous alloys have gained considerable interest in catalysis because of their unique structures and/or chemical properties [9]. A number of amorphous alloys have shown high catalytic performance over various catalytic reactions such as CO hydrogenation, olefin hydrogenation, ammonia synthesis, methanol synthesis and methanation [9]. Recently, new alloy catalysts with supported amorphous structure revealing high surface area (>150 m<sup>2</sup> g<sup>-1</sup>) have been developed [10,11]. Therefore, although amorphization of alloy catalysts is thought to be an available activation treatment, amorphous alloy catalysts cannot be easily prepared by most of the well known method such as melt quenching, vapor and sputter deposition. If amorphous structure could be easily prepared, the method would have the potential to be a further activation treatment of alloy catalysts.

As mentioned above, the HIA treatment on IMCs is a very available method for obtaining amorphous structure, in which we may expect drastic change in surface geometry for catalysis. Catalytic properties of hydrogenated IMCs have been reported in a number of papers but change in catalytic properties along amount of absorbed hydrogen was not investigated.

\* Corresponding author. Tel.: +81 2 2217 5404.

E-mail address: [naruki@mail.tagen.tohoku.ac.jp](mailto:naruki@mail.tagen.tohoku.ac.jp) (N. Endo).

In the present work, we have chosen the C15 Laves  $\text{CeNi}_2$  and investigated its catalytic properties under CO hydrogenation. This paper reports not only the catalytic property for  $\text{CeNi}_2$  after hydrogen absorption but also highlights the possibility of HIA treatment as a new activation method for IMC catalysts.

## 2. Experimental

The  $\text{CeNi}_2$  compound was prepared by arc-melting in an Ar atmosphere. The homogeneity and/or stoichiometry of the inter-metallic compound was characterized by powder X-ray diffraction (XRD). Powder X-ray diffraction was performed with  $\text{Cu K}\alpha$  ( $\lambda = 1.543 \text{ \AA}$ ) radiation and scan step ( $0.02^\circ$ ) by a Mac science M03XHF22 operated at 40 kV and 30 mA. X-ray photoelectron spectroscopy (XPS) experiments were performed on clean surfaces at room temperature under  $10^{-8} \text{ Pa}$  using an Al  $\text{K}\alpha$  monochromated X-ray beam (ESCALAB 220i, Fisons Instruments). The binding energy of 284.5 eV for C1s from surface carbon contaminant was used for the binding energy calibration. All samples for XPS measurements were treated by sputtering (3 kV for 200 s) in order to remove surface contaminants. Specific surface area was measured by the BET method using krypton (Kr) physisorption at  $-196^\circ\text{C}$  (77 K).

The hydrogen absorbed  $\text{CeNi}_2$  was prepared using a standard Sieverts-type apparatus (Suzuki Shokan) for the measurement of pressure–composition–temperature (PCT) curve. The hydrogen absorption condition of HIA was as follows; the hydrogen pressure was increased to 0.34 MPa taking 3 h from a vacuum state at room temperature. The holding time was more than 12 h to prepare considerable amorphous sample ( $\sim 5.0 \text{ g}$ ). As for disproportionation, the initial hydrogen pressure was 2 MPa at  $250^\circ\text{C}$  for 1 h, and then hydrogen pressure was raised up to 4 MPa and held at  $400^\circ\text{C}$  for 24 h. Hydrogen absorption was carried out after the activation treatment under vacuum at  $400^\circ\text{C}$  for 1 h.

The reaction did proceed in a standard fixed-bed flow reactor while a mixture gas of  $\text{H}_2/\text{CO}=2$ ;  $\text{CO}=33.6\%$  at a total flow rate of  $1.5 \text{ ml min}^{-1}$  and total pressure of 0.101 MPa (1 atm) over the catalyst of 500 mg (100 mg for  $\text{CeO}_2$ ). All the catalytic experi-

ments were carried out on the fresh samples without any reduction pretreatment. The reaction products were monitored by on-line gas chromatographs (Shimadzu GC-8A and GC-9A) equipped with Molecular Sieve 5A for the detection of  $\text{H}_2/\text{CO}/\text{CH}_4$  and Porapak Q to detect C2–C4 hydrocarbons and  $\text{H}_2\text{O}$ . The selectivity (C-%) was calculated based from

$$S_i = \frac{(C_i \times i)}{\sum_i^n} \times 100 \quad (1)$$

where  $S_i$  is the selectivity of the  $i$ th product and  $C_i$  is the formation rate of the  $i$ th product ( $\text{mol min}^{-1}$ ),  $n$  is the number of products [12]. The measured data of the catalytic activity were recorded after the reaction achieved a steady state for 30 min and 60 min. The catalytic activity and selectivity of all samples were almost the same values after between 30 min and 60 min.

## 3. Results and discussion

Fig. 1(A) shows XRD patterns for (a)  $\text{CeNi}_2$  (Laves cat.), (b)  $\text{CeNi}_2\text{H}_x$  with HIA (HIA cat.) and (c)  $\text{CeNi}_2\text{H}_x$  with disproportionation (Disprop. cat.). The XRD pattern of (a)  $\text{CeNi}_2$  could be well indexed as the C15 Laves phase. The XRD pattern of (c)  $\text{CeNi}_2\text{H}_x$  with disproportionation was assigned to be Ce hydride and  $\text{CeNi}_5$  [13]. For (b)  $\text{CeNi}_2\text{H}_x$  with HIA, Bragg peaks almost disappeared due to HIA. The BET surface area ( $a_{\text{S, BET}}$ ) of  $\text{CeNi}_2$ ,  $\text{CeNi}_2\text{H}_x$  with disproportionation and  $\text{CeNi}_2\text{H}_x$  with HIA were estimated to be 0.13, 0.34 and  $0.17 \text{ m}^2 \text{ g}^{-1}$ , respectively (see Table 1). Generally, hydrogen embrittlement is accompanied in hydrogenated IMCs [14] and hence the highest surface area of  $\text{CeNi}_2\text{H}_x$  with disproportionation is attributed to the embrittlement induced under a severer hydrogen absorption condition. Hereafter, we name the  $\text{CeNi}_2$ , the  $\text{CeNi}_2\text{H}_x$  with HIA and the  $\text{CeNi}_2\text{H}_x$  with disproportionation as Laves cat., HIA cat. and Disprop. cat.

Fig. 2 shows the reaction rate of CO as a function of temperature over four catalysts together with Ni powder ( $a_{\text{S, BET}} = 0.45 \text{ m}^2 \text{ g}^{-1}$ ) and  $\text{CeO}_2$  ( $a_{\text{S, BET}} = 63.0 \text{ m}^2 \text{ g}^{-1}$ ) for references. The activity of HIA cat. with respect to a real rate ( $\mu\text{mol min}^{-1} \text{ m}^{-2}_{\text{cat}}$ ) was the highest among the catalysts, while the Disprop. cat. exhibited a very low

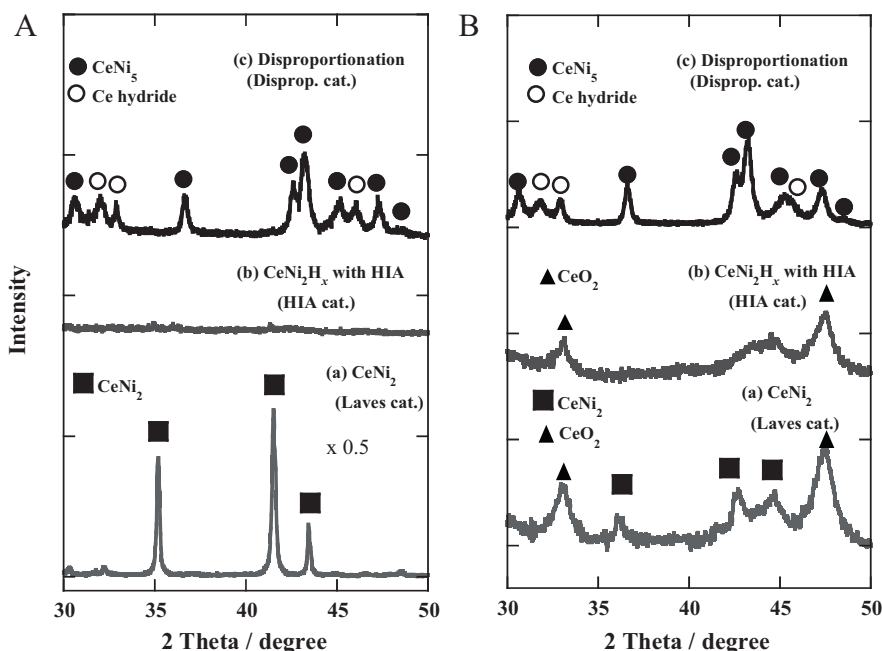


**Fig. 1.** XRD patterns for (a)  $\text{CeNi}_2$  before hydrogen absorption (Laves cat.), (b)  $\text{CeNi}_2\text{H}_x$  with HIA (HIA cat.) and (c)  $\text{CeNi}_2\text{H}_x$  with disproportionation (Disprop. cat.) before (A)/after CO hydrogenation (B).

**Table 1**  
Phase of each sample and surface area before/after CO hydrogenation.

Sample	Phase	Surface area ( $\text{m}^2 \text{g}^{-1}$ )	
		Before	After
Ni powder	Crystal (pure nickel)	0.45	0.45
Laves cat. <sup>a</sup>	Crystal (C15 Laves type)	0.13	0.10
HIA cat. <sup>b</sup>	Amorphous (HIA)	0.17	0.17
Disprop.cat. <sup>c</sup>	Crystal ( $\text{CeNi}_5$ + Ce hydride)	0.34	0.12

<sup>a</sup> CeNi<sub>2</sub> before hydrogen absorption.

<sup>b</sup> CeNi<sub>2</sub>H<sub>x</sub> with HIA.

<sup>c</sup> Disproportionation

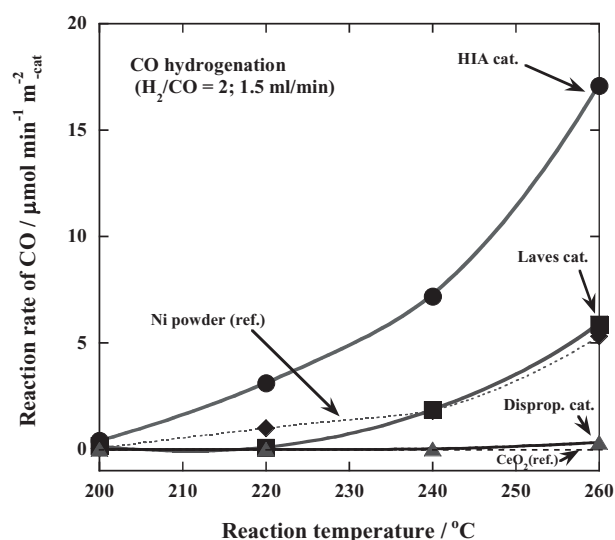


**Fig. 2.** Reaction rate of CO as a function of reaction temperature over five catalysts (0.50 g). Laves cat. ( $\text{CeNi}_2$ ), HIA cat. ( $\text{CeNi}_2\text{H}_x$  with HIA), Disprop. cat. (Disproportionation), Ni powder (ref.) and  $\text{CeO}_2$  (ref.) in terms of ( $\mu\text{mol min}^{-1} \text{m}^{-2}_{\text{cat}}$ ); under a mixture gas of CO (33.6 vol.%) +  $\text{H}_2$  (66.4 vol.%); flow rate:  $1.5 \text{ ml min}^{-1}$ .

activity. The activity of HIA cat. was much higher than that of Ni powder with respect to its surface area, being almost three times higher than the HIA cat. These results imply that the difference in activity of these catalysts depend on not only the surface area but also their inherent structures. Here,  $\text{CeO}_2$  for reference exhibited no activity in this reaction temperatures range in spite of its extremely high surface area.

Fig. 3 exhibits the selectivity in CO hydrogenation with respect to the value of CO conversion on three different catalysts as a function of reaction temperature. The methane (C1) selectivity of Ni powder exhibited almost 90 C-% independent of temperature for reference. In the case of Laves cat. (Fig. 3(A)), the C1 selectivity decreased with increasing temperature, whereas, the C2 and C3 selectivity increased with an increment in temperature. All C2 hydrocarbons were ethane in each sample. The amount of C3 hydrocarbon was almost the same as that of propylene and propane. For HIA cat. in Fig. 3(B), the C1 selectivity also decreased with increasing temperature and the C4 hydrocarbons, butane, formed at reaction temperatures over  $260^\circ\text{C}$ . The C3 hydrocarbons in the case of the HIA cat. was only propane. Regarding the selectivity of Disprop. cat., in contrast, the C1 selectivity was higher than that of the other two. Here, in order to compare each selectivity under the similar conversion, we focused on the selectivity at 260, 240 and  $280^\circ\text{C}$  for Laves cat., HIA cat. and Disprop. cat., respectively. For both Laves and HIA cat., the C1 selectivity is almost the same. However, the C3 hydrocarbons of former were propylene and propane, whereas, those of latter were all propane as mention above. In the case of the Disprop. cat., the amount of propylene was about 70% in C3 hydrocarbons. Moreover, the C4 hydrocarbons were formed only in the case of HIA cat. The other two catalysts could not produce C4 hydrocarbon completely even at higher conversion region or/and at reaction temperatures higher than  $280^\circ\text{C}$ . Therefore, the selectivity is completely different among three catalysts. Except Ni powder no formation of water ( $\text{H}_2\text{O}$ ) was detected under CO hydrogenation on the compound and hydrides, we consider that these catalysts were oxidized under the reaction.

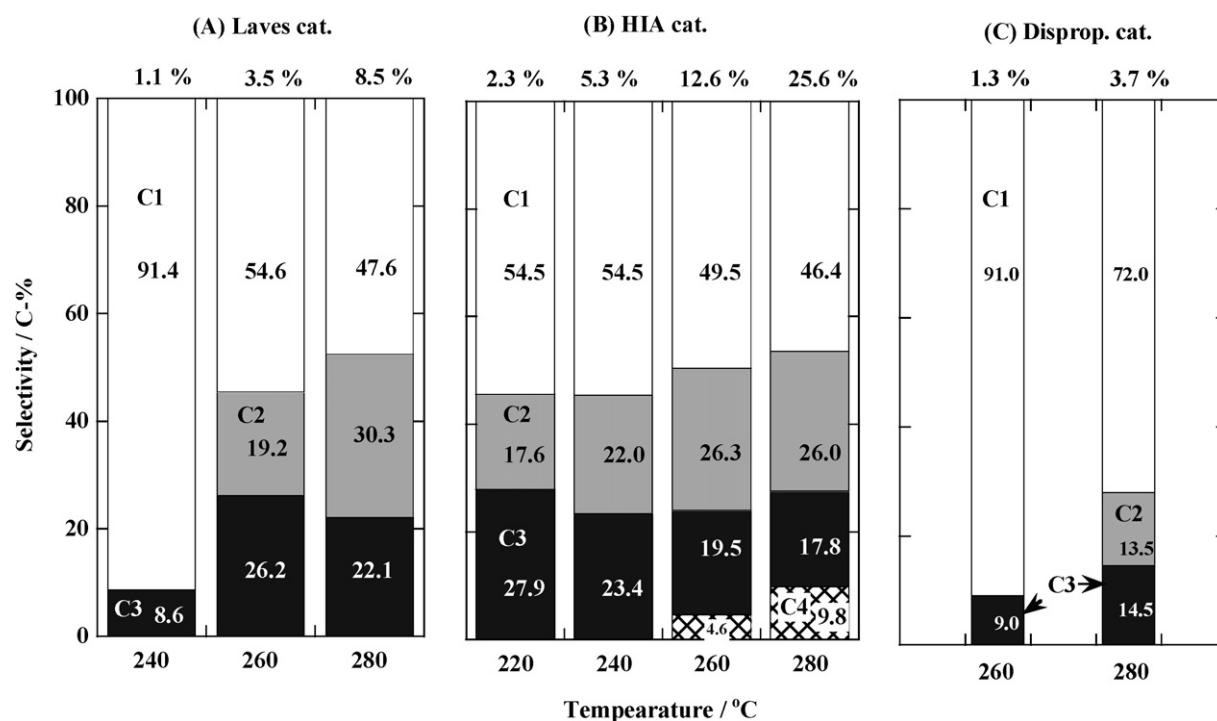


**Fig. 3.** Selectivity (C-%) in the reaction of CO hydrogenation with respect to the value of CO conversion (%) on the three different catalysts (Laves cat. ( $\text{CeNi}_2$ ), HIA cat. ( $\text{CeNi}_2\text{H}_x$  with HIA) and Disprop. cat. (Disproportionation)), depending on reaction temperature.

The XRD patterns of (a) Laves cat., (b) HIA cat. and (c) Disprop. cat. after the reaction are shown in Fig. 1(B). In the XRD pattern for Laves cat. and HIA cat., the diffraction peaks of CeO<sub>2</sub> were observed due to the oxidation of these catalysts. On the other hand, the XRD pattern for Disprop. cat. remained the same even after the reaction because of its extremely low activity. For Laves cat., from the decrease in intensity of CeNi<sub>2</sub> peaks (■) and no occurrence of any other peak of Ce–Ni IMCs, it is supposed that HIA occurred during the reaction as well as the oxidation [13]. For HIA cat., unidentified broad diffraction peaks were observed around 45° which may be generated from the nickel (and cerium) oxide nano-composited phases. The diffraction peak at 43.4° is responsible for NiO [15].

The results of BET measurements for Laves cat., HIA cat. and Disprop. cat. after the reaction are also shown in Table 1. The surface area of Disprop. cat. decreased after the reaction, while the surface areas of other samples remained no change. Though the difference in reaction rate among these catalysts is larger than those in the surface area, the difference of catalytic activity mainly depends on the surface structures. The surface nickel concentrations which were determined by XPS measurement of Laves cat., HIA cat. and Disprop. cat. after the reaction were 24.9, 24.1 and 16.0 at%, respectively. It should be noticed that the surface nickel concentration of Laves cat. was very close to that of HIA cat. From this result and Fig. 1(B), it is presumable that the surface structures of Laves cat. and HIA cat. were modified to the similar structure during CO hydrogenation.

The HIA cat. was found to exhibit the high catalytic activity and the high selectivity of C<sub>2</sub>+ hydrocarbons for the CO hydrogenation. The high catalytic performance of the amorphous alloys has been reported so far [9]. It is well known that the surface of amorphous materials should be devoid of any long-range ordering of constituents and exhibit a high density of low-coordination sites and defects in catalysts, *i.e.* step and edge sites [16,17]. Therefore, the amorphous structure of HIA cat. would play an important role for the high activity. Additionally, we should consider the contribution of the nano-composited NiO+CeO<sub>2</sub> phase for the reaction since the oxidation of HIA cat. proceeds during the CO hydrogenation (Fig. 1(B)). It should be noticed that we could not exclude the possibility that very fine particles of Ni metal are located on the surface as active sites. On the other hand, selectivity for the CO hydrogenation is supposedly strongly depending on the surface structure because the selectivity of products was much different between HIA cat. and Disprop. cat. (Fig. 3). The process of C–O dissociation/hydrogenation followed by stabilization of intermediates such as CH<sub>x</sub> (a) species and formation of C<sub>2</sub>+ hydrocarbons may be enhanced significantly over the HIA cat., *i.e.* inhibition of the methanation process. The characterization of these catalysts and investigation of surface structures are under study.

Although oxidation of CeNi<sub>2</sub> and hydrides could not be avoided under CO hydrogenation, each catalytic performance was different and it is interesting to study how catalytic properties of these catalysts would exhibit for other catalytic reactions. A favorable reaction of HIA catalyst could be oxygen-free reaction system, such as olefin hydrogenation [18]. In this paper, we firstly reported

the different catalytic property by the structure in CeNi<sub>2</sub> and its hydrides. It is also highlighted that HIA treatment is promising as a new activation treatment for IMC catalysts.

#### 4. Conclusions

We have investigated the catalytic properties for CO hydrogenation of C15 Laves intermetallic compound CeNi<sub>2</sub>, which underwent some remarkable change in its structure by hydrogen absorption and temperature, *i.e.* hydrogen-induced amorphization (HIA) and disproportionation. The amount of amorphous and disproportionation catalysts could be controlled by hydrogen absorption. Although the oxidation of CeNi<sub>2</sub> and CeNi<sub>2</sub>H<sub>x</sub> with HIA occurred under the reaction, its catalytic property (activity and selectivity) showed completely different from one another. These results indicated their catalytic property mainly depended on the bulk structure. Especially, the HIA cat. exhibited the highest activity and the unique selectivity. This study reports the possibility of HIA treatment being a new activation process for intermetallic compound for catalysts.

#### Acknowledgements

We are grateful to Dr. Y. Xu at National Institute for Materials Science (NIMS) for helping in performing the BET measurement. This work was supported in part by Grants-in-Aid for Scientific Research (A) 19206072 and Global COE Program “Materials Integration International Center of Education and Research, Tohoku University,” Ministry of Education, Culture, Sports, Science and Technology (MEXT), Japan.

#### References

- [1] K. Kovnir, M. Armbüster, D. Teschner, T.V. Venkov, F.C. Jentoft, A. Knop-Gericke, Yu.-Grin, R. Schlögl, *Sci. Technol. Adv. Mater.* 8 (2007) 420.
- [2] T. Komatsu, A. Onda, *Catal. Surv. Asia* 12 (2008) 6.
- [3] J.C. Bauer, X. Chen, Q. Liu, T.H. Phon, R.E. Schaak, *J. Mater. Chem.* 18 (2008) 275.
- [4] T. Komatsu, D. Sato, A. Onda, *Chem. Commun.* (2001) 1080.
- [5] S. Kameoka, A.P. Tsai, *Catal. Today* 132 (2008) 88.
- [6] N. Endo, S. Kameoka, A.P. Tsai, T. Hirata, C. Nishimura, *Catal. Lett.* 139 (2010) 67.
- [7] For example K. Aoki, T. Yamamoto, T. Masumoto, *Scripta Metall.* 21 (1987) 27.
- [8] X.-G. Li, Ph.D. Dissertation, Tohoku University, 1993.
- [9] A. Baiker; M. Graziani, C.N.R. Rao (Eds.) *Advance in Catalyst Design*, Singapore, 1992, p.217;
- [10] A. Baiker, *Topics of Applied Physics: Glassy Metals 3*, vol. 72, Springer, 1994, p. 121.
- [11] J. Young, Ph.D. Dissertation, Fudan University, 1993.
- [12] J.-F. Deng, H. Li, W. Wang, *Catal. Today* 51 (1999) 113.
- [13] G. Kisfaludi, K. Lázár, Z. Shay, L. Gucci, Cs. Fetzter, G. Konczos, A. Lovas, *Appl. Surf. Sci.* 24 (1985) 225.
- [14] V. Paul-Boncour, C. Lartigue, A. Percheron-Guegan, J.C. Achard, J. Pannetier, *J. Less-Common Met.* 143 (1988) 301.
- [15] M. Nugamo, *Zairyo-to-Kankyo* 56 (2007) 132.
- [16] K. Nakahigasi, Y. Shimomura, N. Fukuda, *Acta Crystallogr. A* 28A (1972) S234.
- [17] G.V. Smith, O. Zahaa, Á. Molnár, M.M. Kahn, B. Lichter, W.E. Brower, *J. Catal.* 83 (1983) 238.
- [18] G.V. Smith, Á. Molnár, M.M. Kahn, D. Ostrgrad, N. Yoshida, *J. Catal.* 98 (1986) 502.
- [19] N. Endo, S. Ito, K. Tomishige, S. Kameoka, A.P. Tsai, T. Hirata, C. Nishimura, *Catal. Catal. (Shokubai)* 52 (2010) 369.